energies

MDPI

Article

A Three-Dimensional Orthogonal Receiving Coil for In Vivo Microrobot Wireless Power Transmission Systems

Ding Han [1,2,*], Guozheng Yan [1,2], Pingping Jiang [1,2], Zhiwu Wang [1,2] and Wei Wang [1,2,*]

[1] School of Electronic Information and Electrical Engineering, Shanghai Jiao Tong University, Shanghai 200240, China
[2] Shanghai Engineering Research Center of Intelligent Addiction Treatment and Rehabilitation, Shanghai 200240, China
* Correspondence: tinkling@sjtu.edu.cn (D.H.); w775276998@163.com (W.W.)

Abstract: Approaches to studying electromagnetic induction in weak coupling have recently received attention in robotics since they could be used to supply energy to robots, allowing robots to diagnose and treat diseases in the human body. A three-dimensional orthogonal receiving coil connected in parallel, with a size of 13 mm × 13 mm × 13 mm, for an intestinal examination microrobot is designed in this article. Based on the defined attitude functions, we build and verify the stability and effectiveness of the proposed coil model through both analytical calculation and simulation analysis. In addition, to supply enough power to the microrobot, the number of turns of the receiving coil is optimized, considering both the electrical coil parameters and the limited space inside the robot. Then, an evaluation of the proposed 3D orthogonal receiving coil is presented in the bench tests. The results show that the power transmission efficiency can reach as high as 9.6%, with 1271 mW. This paper also uses a curved pipe to simulate the robot's movement with the designed coil in the tortuous intestine. The average speed is 0.97 mm/s, with the path covering 180°. The experiments illustrate the excellent performance of the wireless power transmission, even when the positions of the two induction coils are constantly changing.

Keywords: in vivo microrobot; wireless power transmission; receiving coil; attitude functions

check for updates

Citation: Han, D.; Yan, G.; Jiang, P.; Wang, Z.; Wang, W. A Three-Dimensional Orthogonal Receiving Coil for In Vivo Microrobot Wireless Power Transmission Systems. *Energies* **2022**, *15*, 6321. https://doi.org/10.3390/en15176321

Academic Editor: Alon Kuperman

Received: 4 August 2022
Accepted: 24 August 2022
Published: 30 August 2022

Publisher's Note: MDPI stays neutral with regard to jurisdictional claims in published maps and institutional affiliations.

Copyright: © 2022 by the authors. Licensee MDPI, Basel, Switzerland. This article is an open access article distributed under the terms and conditions of the Creative Commons Attribution (CC BY) license (https://creativecommons.org/licenses/by/4.0/).

1. Introduction

Due to the advantages of minimally invasive or non-invasive detection in the body, gastrointestinal doctors and bioengineering researchers all around the world have recently paid more attention to capsule endoscopes [1–3]. Capsule endoscopes can be more friendly to patients than traditional endoscopes [4]. Currently, the clinical endoscope uses a button battery, which can only provide an average of 25 mW of energy for 6 to 8 h. This is only enough to collect images of the digestive tract at a rate of 2 frames/s [5]. In addition, because capsule endoscopes move passively with intestinal peristalsis, missed detections often occur. Thus, microrobots with active intestinal disease detection movement have become a research trend [6].

With the functions of active motion, fixed-point sampling, drug delivery, and so on, the power consumption of the microrobot is high, reaching 580 mW [7]. The button battery obviously cannot supply enough power. Power supply using cables is also invalid since they barely cover the whole intestine and may cause damage to the intestine. An effective way to realize non-contact energy transmission through human tissue is needed to address these issues.

Considering that the robot only moves within a range of about 20 cm × 20 cm of the human abdomen, Lenaerts et al. [8] of the University of Leuven in Belgium proposed in 2005 to use a wireless power transmission technology, based on the principle of near-field inductive coupling, to power the robot. That is, a transmitting coil that can excite an alternating magnetic field in the abdominal region of the human body is placed outside

the body, and a receiving coil integrated into the robot can obtain energy based on an inductive electromotive force. After more than ten years of research, wireless power transmission (WPT) technology has been recognized as the most desirable solution to the energy supply problems of in vivo microrobots. Furthermore, miniaturization technology makes it possible for the coil to be used in microdevices [9].

Recently, researchers have investigated wireless power transmission systems in particular to solve the problems of energy supply to robots. In the research of [10], the researchers proposed segmented solenoid coils at the transmitting end. In order to reduce the mutual inductance distance between the transmitting and receiving coils, the designed coils were placed on the surface of the human body. The results showed that the average power transmission efficiency (PTE) was 3.8%. However, on the one hand, the uniformity of the magnetic field was not discussed nor guaranteed. On the other hand, the electromagnetic safety distance was ignored in the research. The work of [11] demonstrated the usefulness of the classic Helmholtz coil pair. The Helmholtz coil pair is a device in which two identical coils are separated by a distance equivalent to the radius of the circular loops. Due to the open space in the Helmholtz coil, other instruments can be easily inserted or removed. More importantly, a uniform magnetic field could be created using Helmholtz coils [12,13]. However, the one-dimensional receiving coil only supplied low power. The approach to optimizing wireless power transmission systems reviewed in [14,15] is based on a three-coil wireless power transmission system. In this work, a Helmholtz-like load coil structure was applied. The experimental results indicated that the maximum power transfer was over 800 mW at the optimized position between the transmitting and receiving coils. Otherwise, in some other positions, the efficiency of the three-coil system was not improved, and even worsened, due to the enormous power consumption of the coils themselves compared to the two-coil system. Some other approaches, which attempted to optimize the transmitting coil or receiving coil, were only at the bench test stage [16,17]. Further reports on robot experiments have not been conducted. However, the wireless power transmission technology applied to gastrointestinal robots faces new challenges. Firstly, there is a big difference in size between the transmitting coil and the receiving coil, and they are separated by a long distance, resulting in a small coupling coefficient and low efficiency [18–21]. Secondly, the position and posture of the microrobot in the human body are constantly changing. Therefore, it is not easy to achieve complete coupling between the transmitting coil outside of the body and the receiving coil in the body, which affects the energy transmission stability.

In this paper, we propose a novel three-dimensional orthogonal receiving coil for in vivo wireless power transmission systems. Based on the parameter optimization of the proposed receiving coil, the transmission efficiency can be improved. Furthermore, its unique structure guarantees the stability of energy transmission at any position, even with the relative position changing.

This article is organized as follows: Section 2 reviews the working principle of the WPT system for in vivo microrobots; Section 3 shows details of the design and the optimization of the three-dimensional receiving coil; experiments are conducted to validate the stability and effectiveness of the proposed coils in Section 4; and Section 5 draws discussions and conclusions.

2. Wireless Power Transmission for Microrobots

2.1. System Overview

Figure 1 presents the non-invasive intestinal disease detection system. It consists of a wireless power transmission system, a microrobot, a communication unit, and a human–computer interaction system. The wireless power transmission system includes two modules, the transmitting coil module, which is used to supply power placed around the body, and the receiving coil module, equipped in the microrobot for obtaining power. With the energy, the microrobot can move actively in the intestine using the expanding mechanism (EM) and the telescoping mechanism (TM) to capture tissue images and deliver

drugs. Through the communication unit, operators can obtain real-time information about the intestine on the human–computer interaction system for diagnosis and examination.

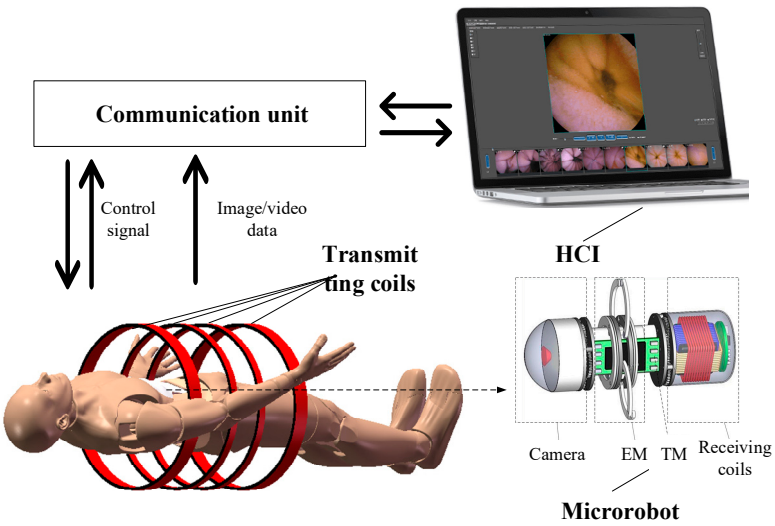


Figure 1. The non-invasive intestinal diseases detection system.

2.2. Working Principle of WPT

The wireless power transmission system supplies energy to the microrobot based on the principle of near-field inductive coupling, as shown in Figure 2. The primary side, also known as the transmitting coil part, excites an alternating magnetic field through the inverter and the resonant circuit. The receiving coil, on the secondary side, utilizes the induced electromotive force to power the robot after the rectifiers and regulator.

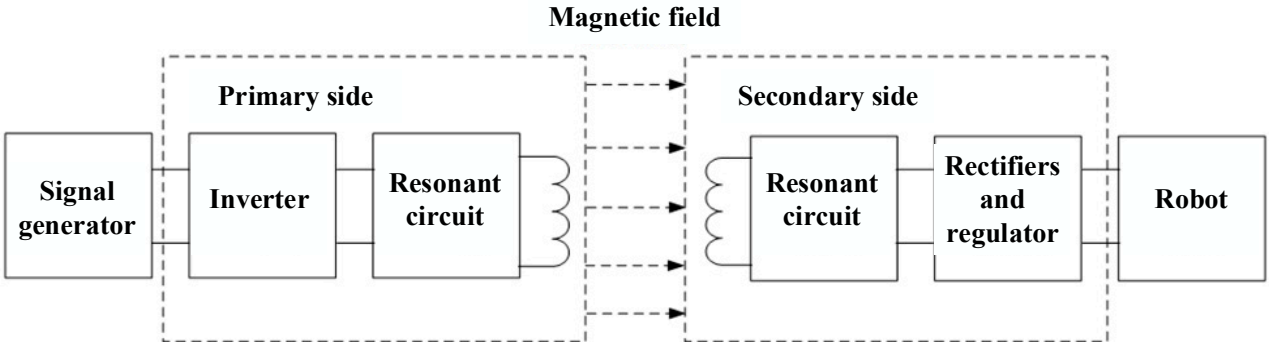


Figure 2. Block diagram of wireless power transmission.

3. Design of Receiving End in WPT

The receiving system in wireless power transmission includes two parts: the RLC series resonant circuit and the energy management circuit. The series resonant circuit, in turn, contains the receiving coil and tuning capacitors, which are used to resonate the receiving circuit. The resonant circuit utilizes the alternating magnetic field (AMF) excited by the transmitting coil to generate induced electromotive force. After the stabilization and rectification of the induced alternating current (AC), the energy management circuit finally provides a stable voltage for the in vivo device. In order to improve the induced electromotive force of the receiving end, a novel 3D orthogonal receiving coil was designed in this study. The mutual inductance M was optimized by analyzing the attitude function. In addition, the selection and optimization of the litz wires used in the winding of the receiving coil were also considered.

3.1. Design of Energy Management Circuit

The energy management circuit consisted of two modules: a rectifier circuit and a voltage regulator circuit. Using the energy management circuit, the alternating current (AC) was turned into a direct current (DC) that offered power to the in vivo devices.

3.1.1. Rectifier Circuit

A full-bridge rectifier was adopted in the energy management circuit. A schematic diagram of the full-bridge rectifier is shown in Figure 3. It was used to convert the AC voltage generated by the receiving coil into pulsating DC voltage for use in power supplies. Small diodes lay in a quad array, which could provide the ability for polarity independence, reverse polarity protection, and low-loss bridge rectification. In addition, its small size (3 mm × 2 mm) and high-energy efficiency are very suitable for in vivo devices such as microrobots for diagnosing intestinal diseases.

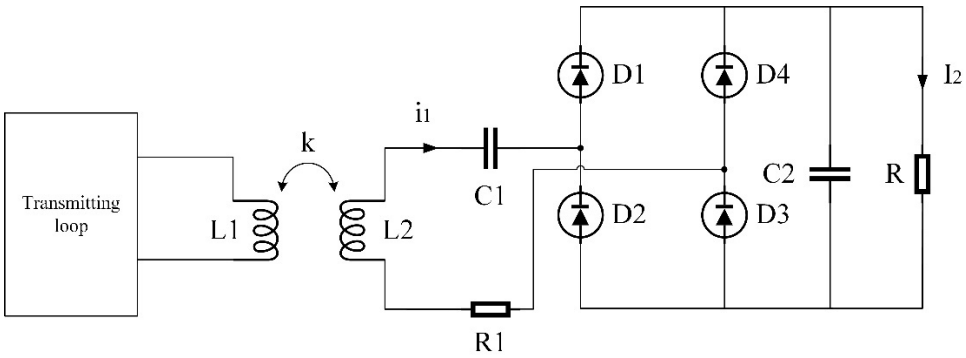


Figure 3. Schematic diagram of the full-bridge rectifier.

3.1.2. Regulator Circuit

The output of the resonant circuit at the receiving end generated a ripple voltage, the amplitude of which was still changing after rectification. It could not be directly connected to the in vivo devices. Note that a voltage regulator circuit was needed to perform voltage regulation. The working voltage of the microrobot system was 3.3 V. Considering the chip size and voltage regulation accuracy, the regulator circuit in the microrobot system was realized by the LT1763 chip packaged in DFN. The size of the chip was 3 mm × 4 mm. A schematic diagram of the regulator circuit based on LT1763 is presented in Figure 4.

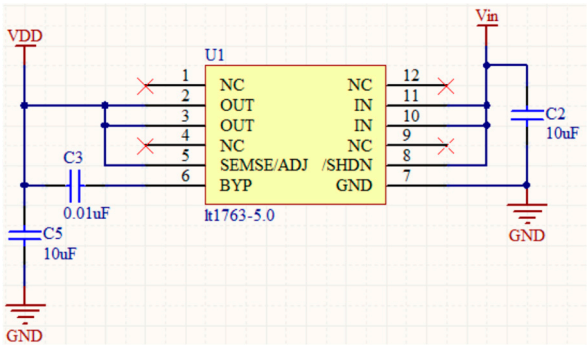


Figure 4. Circuit diagram of the regulator.

The regulator circuit based on LT1763 is a low-power, low-dropout, and low-noise system. The DC voltage noise output by the LT1763 chip is only 20 μ VRMS. Moreover, it has the benefits of reverse battery protection and overcurrent and overtemperature protection. All the details mentioned above indicate the designed system has good stability for the microrobot.

3.2. Design and Optimization of Receiving Coil

The induced electromotive force ε of the receiving coil and the sinusoidal excitation current I_t in the transmitting coil have the following relationship:

$$\varepsilon = M\frac{dI_t}{dt} \tag{1}$$

where M represents the mutual inductance between the transmitting and the receiving coils. Substitute the expression

$$I_t = I_m sin(2\pi ft) \tag{2}$$

into Equation (1), and we can obtain ε', and the root mean square value of ε as

$$\varepsilon' = \sqrt{\frac{1}{T}\int_0^T \varepsilon^2 dt} = \sqrt{2}\pi f M I_m \tag{3}$$

where I_m is the excitation current amplitude and f is the frequency.

From Equation (3), it can be seen that in order to improve the induced electromotive force, the mutual inductance M, the resonant frequency f, and the excitation current I_m should be increased. As features of the transmitting coil such as the resonant frequency f and excitation current I_m are determined, the mutual inductance M plays a key role in enhancing electromotive force.

Considering the attitude of the three-dimensional receiving coil, the mutual inductance M can be defined in terms of attitude function $f(\theta_1, \theta_2)$,

$$M = N_r M_0 f(\theta_1, \theta_2) \tag{4}$$

where N_r is the number of receiving coil turns and M_0 is the single-turn mutual inductance between the receiving coil and the transmitting coil. The details are discussed in Section 3.2.1.

In addition, in Equation (5),

$$M = \frac{\Phi_r}{I} = \frac{B \cdot S_r}{I} \tag{5}$$

we can observe that the mutual inductance is proportional to the receiving coil area S_r. Here, Φ_r is the magnetic flux, and B is the magnetic flux density.

Therefore, the induced electromotive force can be increased by increasing the effective projected area of the receiving coil in the transmitting magnetic field.

3.2.1. 3D Orthogonal Receiving Coil

For an in vivo microrobot, note that the wireless power transmission distance is relatively long. The size difference between the receiving and the transmitting coils is too large. Thus, a ferrite core with bonding wires was adopted to enhance the coupling coefficient [22].

The attitude definition of 1D, 2D orthogonal, and 3D orthogonal receiving coils in the unidirectional alternating magnetic field is shown in Figure 5. The emission magnetic field is distributed along the z-axis. Three sets of coils were, respectively, wound around three sets of orthogonal surfaces of the ferrite core, which formed a 3D orthogonal receiving coil. The rotation angle of the receiving coil around the x-axis was defined as θ_1; likewise, the rotation angle around the y-axis was defined as θ_2. Both θ_1 and θ_2 determine the attitude function. Because the winding directions of the coils in different dimensions have an orthogonal relationship, the induced magnetic fields created by coils in different dimensions do not affect each other.

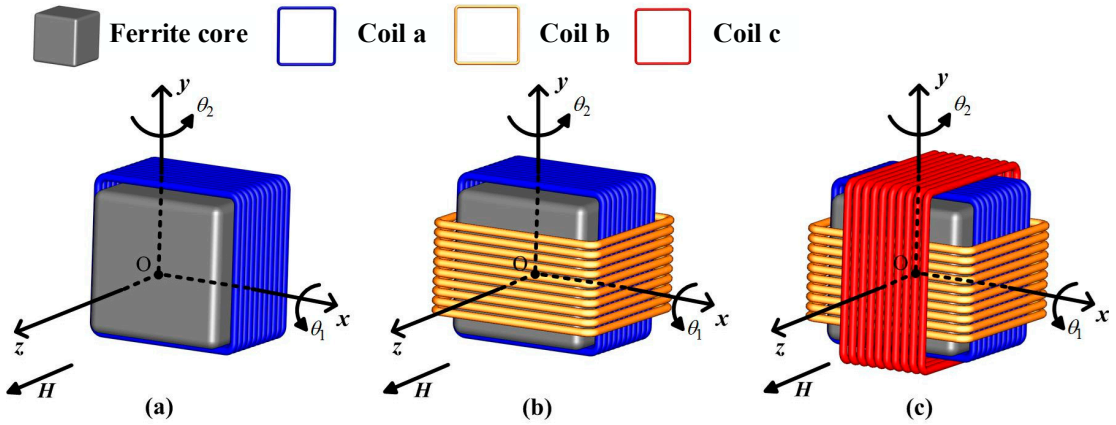


Figure 5. Attitude definition of three-dimensional orthogonal receiving coil. (**a**) One-dimensional orthogonal coil. (**b**) Two-dimensional orthogonal coil. (**c**) Three-dimensional orthogonal coil.

In the patient's body, with the continuous movement of the microrobot, its position and posture are also constantly changing. The relative position of the receiving coil embedded in the robot and the transmitting coil outside the body is also changing. As is known, since electromagnetic energy decays quickly with distance, the misalignment in position and angle plays a key role in inductive coupling. To address this issue, the position and the posture of the receiving coil should be considered.

The attitude function is introduced to quantitatively describe the attitude of the receiving coil. The attitude functions of the coils a, b, and c can be expressed as

$$f_a(\theta_1, \theta_2) = |cos\theta_1 cos\theta_2| \tag{6}$$

$$f_b(\theta_1, \theta_2) = |sin\theta_1 cos\theta_2| \tag{7}$$

$$f_c(\theta_1, \theta_2) = |sin\theta_2| \tag{8}$$

Then, the projected area of the three-dimensional receiving coil with any attitude on XOY is:

$$\begin{cases} {S_a}^{XOY} = S_a \cdot |cos\theta_1 cos\theta_2| = S_a \cdot f_a(\theta_1, \theta_2) \\ {S_b}^{XOY} = S_b \cdot |sin\theta_1 cos\theta_2| = S_b \cdot f_b(\theta_1, \theta_2) \\ {S_c}^{XOY} = S_c \cdot |sin\theta_2| = S_c \cdot f_c(\theta_1, \theta_2) \end{cases} \tag{9}$$

where S_a, S_b, S_c represent the geometric area of coils a, b, and c; ${S_a}^{XOY}, {S_b}^{XOY}, {S_c}^{XOY}$ represent the projection of each coil in the direction of the magnetic field.

Due to symmetry, when $\theta_1, \theta_2 \in [0°, 90°]$, all possible attitudes of the coil can be represented. What can be obtained from Equations (6)–(9) is that, for the arbitrary values of θ_1 and θ_2, at least one of the attitude functions of coils a, b, and c is always non-zero. That is, under any attitude, the three-dimensional orthogonal coil can generate induced electromotive force through electromagnetic induction. For further consideration, receiving coils with more than three dimensions cannot achieve an orthogonal arrangement. Note that there is always a mutual inductance between coils of different dimensions that are non-zero, causing the induced electromotive force of the coils to weaken each other. This is not only unfavorable to the improvement of the inductive energy, but it also causes space waste.

There are two ways to create a three-coil connection.

The equivalent projected area of the proposed three coils connected in series is as follows:

$$\begin{cases} S_{\text{series}} = {S_a}^{XOY} + {S_b}^{XOY} + {S_c}^{XOY} = S_a \cdot f_a(\theta_1, \theta_2) + S_b \cdot f_b(\theta_1, \theta_2) + S_c \cdot f_c(\theta_1, \theta_2) \\ 0 \le \theta_1, \theta_2 \le 90 \end{cases} \tag{10}$$

In the other connection way, the equivalent projected area of the proposed three coils connected in parallel is expressed as

$$\begin{cases} S_{\text{parallel}} = max\left({S_a}^{XOY},\ {S_b}^{XOY}, {S_c}^{XOY}\right) = max(S_a{\cdot}f_a(\theta_1,\theta_2), S_b{\cdot}f_b(\theta_1,\theta_2), S_c{\cdot}f_c(\theta_1,\theta_2)) \\ 0 \le \theta_1, \theta_2 \le 90 \end{cases} \tag{11}$$

In order to simplify the analysis, it can be assumed that the projected area of the three coils is the same, that is $S_a = S_b = S_c$. Then, for series connection, Equation (10) can be rewritten as

$$\begin{aligned} min(S_{\text{series}}) &= S_a{\cdot}min(f_a(\theta_1,\theta_2) + f_b(\theta_1,\theta_2) + f_c(\theta_1,\theta_2)) \\ &= S_a \end{aligned} \tag{12}$$

$$\begin{aligned} max(S_{\text{series}}) &= S_a{\cdot}max(f_a(\theta_1,\theta_2) + f_b(\theta_1,\theta_2) + f_c(\theta_1,\theta_2)) \\ &= \sqrt{3}S_a \end{aligned} \tag{13}$$

For the parallel connection, Equation (11) can be rewritten as

$$\begin{aligned} min\left(S_{\text{parallel}}\right) &= S_a{\cdot}min(f_a(\theta_1,\theta_2), f_b(\theta_1,\theta_2), f_c(\theta_1,\theta_2)) \\ &= \tfrac{\sqrt{3}S_a}{3} \end{aligned} \tag{14}$$

$$\begin{aligned} max\left(S_{\text{parallel}}\right) &= S_a{\cdot}max(f_a(\theta_1,\theta_2), f_b(\theta_1,\theta_2), f_c(\theta_1,\theta_2)) \\ &= S_a \end{aligned} \tag{15}$$

From the preceding discussion, we observe that no matter if the coils are connected in series or in parallel, the ratio of the min/max of the equivalent projected area of the coil is the same as $\sqrt{3}/3$. Furthermore, it can be obtained that the ratio of the min/max receiving power of the 3D orthogonal receiving coil is $\sqrt{3}/3$.

To further discuss in series connection, the induced electromotive force generated by coils a, b, and c were superimposed, as well as the equivalent series resistance. The three rectifiers are always in a working state. That is to say, there are always six diodes conducting, and the rectification loss is large. On the other hand, in a parallel connection, thanks to the unidirectional conduction characteristic of the diodes, only the coil with the largest induced electromotive force generates current, and the other two coils are disconnected. There is only one rectifier working in the circuit. That is, only two diodes are turned on, and the energy loss is small. In addition, the equivalent load resistance of the microrobot is generally lower than 30 Ω, which is smaller than the internal resistance of the receiving coil. Based on the above analysis, the three-dimensional coils were connected in parallel.

The influence of the attitude angle on the attitude function is simulated and shown in Figure 6. It can be obtained that the ratio of minimum/maximum of $f_a + f_b + f_c$ $\left(1/\sqrt{3}\right)$ in the left of Figure 6 is the same as that of $\max[f_a, f_b, f_c]$ $((\sqrt{3}/3)/1)$ in the right of Figure 6. This verifies the discussion results of the algebraic derivation.

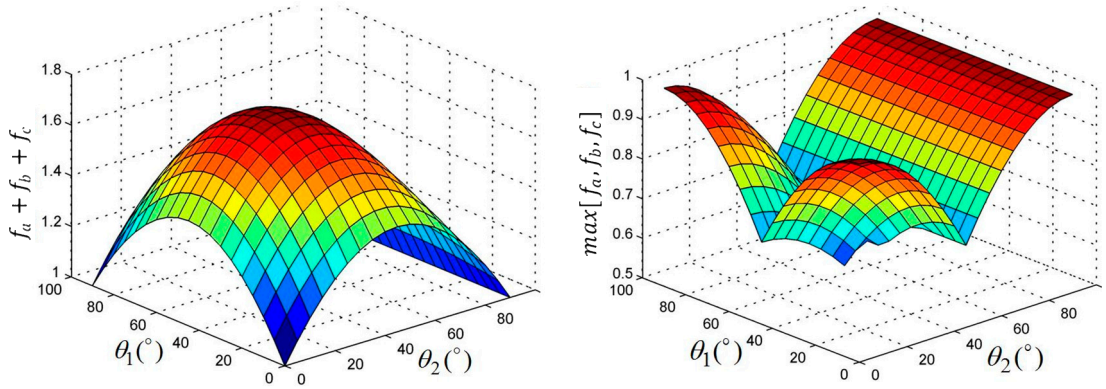


Figure 6. Changing the attitude function of 3D receiving coil using attitude angle.

3.2.2. Optimization of 3D Coils

Litz wires were wound on a cube of ferrite core, forming the 3D receiving coil. The litz wire had six strands, and the diameter of each strand was 0.02 mm. Figure 7 shows the prototype of the receiving coil. Considering the microrobot size constraints, the coil width of each dimension should be less than 13 mm.

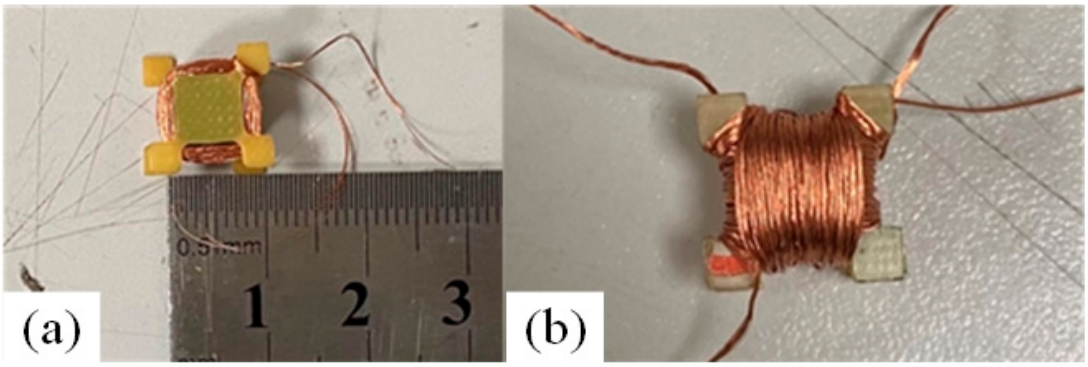


Figure 7. The prototype of receiving coil. (**a**) Finished product of first-dimensional receiving coil. (**b**) Finished product of three-dimensional receiving coil.

In the optimization process, the influence of the number of turns of the receiving coil on coil quality was studied. An impedance analyzer was used to measure the receiving coil's features, such as the equivalent series resistance *R*, equivalent inductance L, and quality factor Q. Then, the relationship between the parameters and the number of turns of the coil could be analyzed. A series of tests were conducted, in which the number of turns ranged from 40 to 130 with an interval of 10 turns. The results are displayed in Figure 8. Note that the vertical axis of this plot is scaled logarithmically for good visualization in this figure.

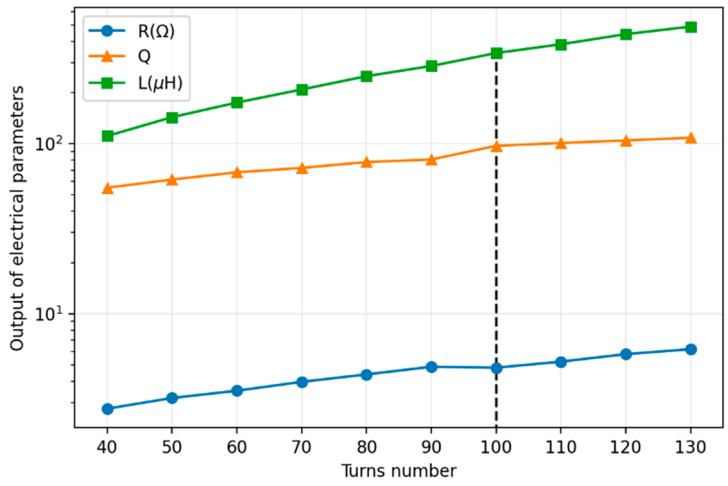


Figure 8. The relationship between the electrical parameters of the receiving coil and the number of turns.

In Figure 8, it can be seen that the parameters such as the equivalent series resistance *R*, equivalent inductance L, and quality factor Q of the coil are positively correlated with the number of turns. From Equation (4), it can be found that more turns of the receiving coil leads to a greater mutual inductance and a greater induced electromotive force in the receiving coil. However, with the number of turns increasing, the equivalent series resistance *R* increases. Moreover, the increase in size cannot be ignored either. For a comprehensive consideration, the number of turns of the single-dimensional coil was determined as 100 turns.

The features of the proposed coil after optimization are listed in Table 1.

Table 1. Design parameters of the 3D receiving coil.

Parameters	Coil *a*	Coil *b*	Coil *c*
$R(\Omega)$	3.73	3.86	4.28
$L(\mu H)$	321.43	317.75	329.02
Q	96.27	96.61	97.57
Wire	Litz wire with 6 strands, 0.12 mm diameter for each strand		
Ferrite core	Cube with size 7 mm × 7 mm × 7 mm, R6K		

4. Experiments

4.1. Bench Tests

The proposed receiving coil with the optimized parameters was made and used in the experiments to verify the reliability of its power supply. The test platform was conducted as shown in Figure 9. The Helmholtz coil, which has been verified to generate a magnetic field with high strength and uniformity [23], was adopted for the transmitting coil. The parameters of the transmitting coil are listed in Table 2. The receiving coil, fixed on a rotatable mechanism, was placed in the middle of the transmitting coil. The receiving coil could realize the rotation movement around the X and Y axes. The equivalent load of the microrobot was replaced by a 30 Ω resistor. The drive voltage was adjusted to 11 V, the current in the transmitting coil was set to 1.2 A, and the frequency was set to 220 kHz.

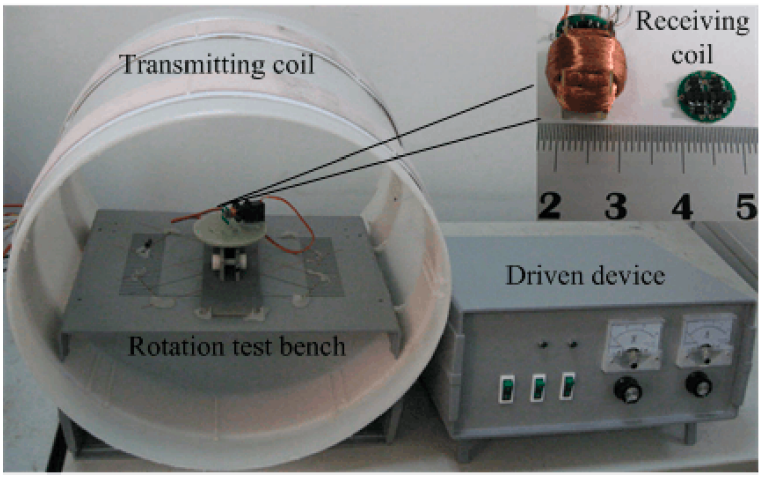


Figure 9. Wireless energy transmission test platform.

Table 2. Parameters of transmitting coil.

Parameters	Value
Diameter/mm	400
Turns No.	20
Wire	Litz wire with 180 strands, 0.12 mm diameter for each strand

As described in the previous section, both θ_1 and θ_2 were controlled to rotate (to simulate a robot at any position in the intestine) from 0° to 90° at a regular interval of 5°, respectively. The receiving power at each attitude was recorded and calculated. Figure 10 displays only parts of the typical values. Note that 0° and 45° are the typical positions due to symmetry. The measured values and the theoretical values had consistent trends. Furthermore, there was only a slight deviation. This is because the size of each dimension of the actual hand-wound coil was not precisely the same. Although unavoidable, this is acceptable. In addition, the discrete interval of 5° may be another small influencing factor.

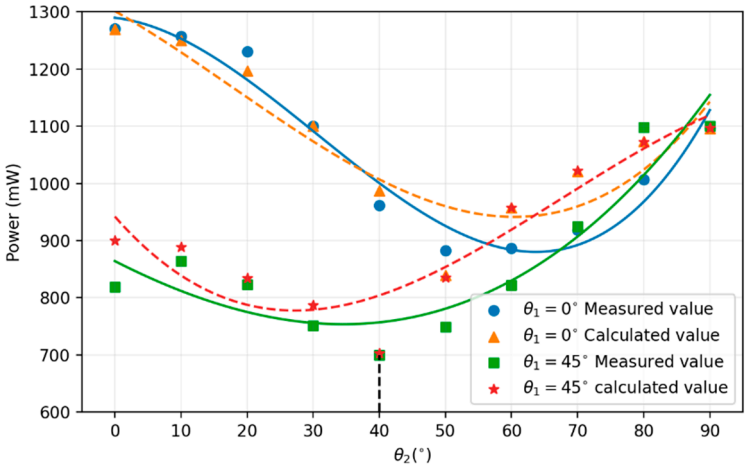


Figure 10. Received power at various attitudes.

The maximum received power of 1271 mW was obtained at $\theta_1 = 0°, \theta_2 = 0°$. Additionally, the minimum power of 700 mW was obtained at $\theta_1 = 45°, \theta_2 = 40°$. It can be found that the ratio of maximum and minimum power was 0.55, which is basically consistent with the theoretical analysis result: $1/\sqrt{3}$. Moreover, the power of the proposed receiving coil supply, at any attitude, meets the 580 mW required by the robot. At any attitude of the receiving coil, its minimum transmission efficiency is 5.3%. Furthermore, its maximum transmission efficiency can reach 9.6%.

4.2. In Vitro Experiments

We implemented the aforementioned 3D orthogonal receiving coil in a microrobot. The proposed receiving coil was equipped at the robot's rear, with the resonance and rectifying circuit connecting nine 100 µF tantalum capacitors in parallel (see Figure 11).

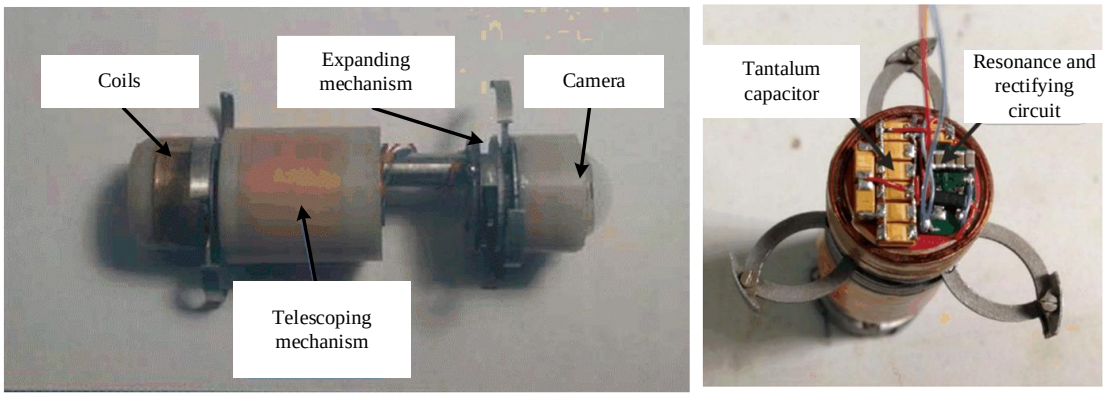
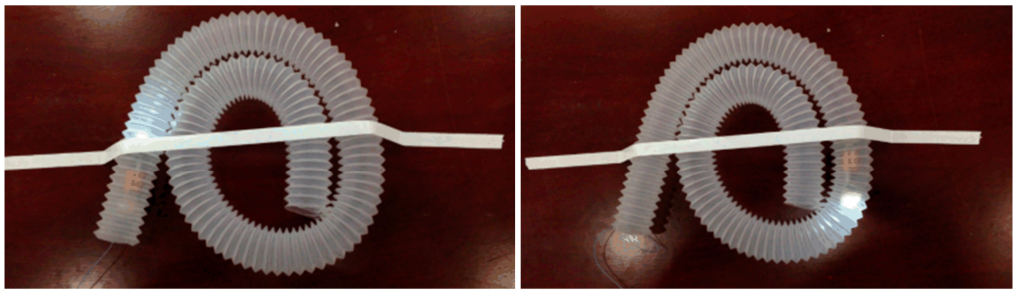


Figure 11. Prototype of the microrobot with proposed receiving coils.

In in vitro experiments, in order to validate the reliability and validity of the designed receiving coil, the robot was placed in a curved pipe under the wireless power transmission conditions. Figure 12 shows the movement experiment of the robot in a curved pipe. With the power supplied by wireless power transmission, the robot was driven to move 200 mm (180°). During the process, different robot attitudes (receiving coil attitudes towards the transmitting coil) were simulated. Five tests were conducted, and the time spent was recorded. The results are listed in Table 3. The average speed was obtained as 0.97 mm/s, and the average time was 205.7 s. The movement experiments illustrated a good performance for wireless power transmission, even when the positions of the two induction coils were constantly changing.



(a) (b)

Figure 12. Performance test of the prototype in a curved pipe. (**a**) the start and (**b**) the turning.

Table 3. Time of 200 mm movement.

	1st	2nd	3rd	4th	5th	Average
Spending time (s)	208.5	205.16	204.46	207.38	203.18	205.7

5. Discussion and Conclusions

Approaches to studying electromagnetic induction in weak coupling have recently received attention in robotics since they could allow robots to diagnose and treat diseases in the human body. Recent work has approached the problem of wireless power transmission for in vivo devices under the assumption that the positions of both the transmitting coil and the receiving coil are fixed. However, we focused on the dynamic wireless power transmission (all time-varying, relative positions between the two coils) since a microrobot with a receiving coil in the intestine moves all the time for disease detection. Unlike previous wireless power transmission systems, which used a one-dimensional coil to receive energy, we constructed a three-dimensional receiving coil, which could sufficiently maintain mutual inductance with the transmitting coil at any attitude. Then, we implemented the proposed coil in a microrobot for diagnosing intestinal diseases.

Firstly, we proposed attitude functions to analyze the misalignment in position and angle. Instead of investigating the induced electromotive force that the WPT system supplied, the equivalent projected area model in the direction of the magnetic field was studied. The algebraic model demonstrates that the ratio of the minimum/maximum received power of the 3D orthogonal receiving coil was $\sqrt{3}/3$. In order to supply enough power to the microrobot in vivo, three-dimensional coils were chosen to be connected in parallel. Then, the reliability of the analysis model was verified by simulation. Secondly, the number of turns of the receiving coil, which plays a pivotal role in coil quality, was optimized considering both the coil's electrical parameters and the limited space in the robot. In addition, a ferrite core was adopted to enhance the coupling coefficient. Finally, bench tests and in vitro experiments using the microrobot were used to evaluate the proposed 3D orthogonal receiving coil. In the bench tests, both attitudes of coils θ_1 and θ_2 were controlled to rotate from 0° to 90°, respectively, simulating the robot at any position in the intestine. The results show that the ratio of maximum 1271 mW and minimum power 700 mW was 0.55, which is consistent with the theoretical analysis result: $1/\sqrt{3}$. Moreover, the power of the proposed receiving coil supply at any attitude meets the 580 mW required by the robot. Furthermore, its maximum transmission efficiency is 9.6%, which is more attractive than the 7.8% presented in the most recent research [24]. In addition, a curved pipe was used to simulate a robot with a 3D coil moving in the intestine. The average speed was 0.97 mm/s, with the path covering 180°. The movement experiments also illustrate the excellent performance of the wireless power transmission, even when the positions of the two induction coils are constantly changing.

Author Contributions: Conceptualization, D.H.; Data curation, P.J.; Funding acquisition, D.H., G.Y. and P.J.; Investigation, G.Y.; Methodology, D.H.; Software, W.W.; Validation, Z.W.; Writing—original draft, D.H.; Writing—review & editing, G.Y. and W.W. All authors have read and agreed to the published version of the manuscript.

Funding: This research was funded by the National Natural Science Foundation of China (62103263; 81971767), the Shanghai Science and Technology Support Project (19142203800), the Natural Science Foundation of Shanghai (21ZR1429900), and Shanghai Engineering Research Center (19DZ2255200).

Institutional Review Board Statement: Not applicable.

Informed Consent Statement: Not applicable.

Data Availability Statement: Not applicable.

Conflicts of Interest: The authors declare no conflict of interest.

References

1. Yang, Y. The future of capsule endoscopy: The role of artificial intelligence and other technical advancements. *Clin. Endosc.* **2020**, *53*, 387. [CrossRef] [PubMed]
2. Hosoe, N.; Kamiya, K.J.L.L.; Hayashi, Y.; Sujino, T.; Ogata, H.; Kanai, T. Current status of colon capsule endoscopy. *Dig. Endosc.* **2021**, *33*, 529–537. [CrossRef] [PubMed]
3. Hosoe, N.; Takabayashi, K.; Ogata, H.; Kanai, T. Capsule endoscopy for small-intestinal disorders: Current status. *Dig. Endosc.* **2019**, *31*, 498–507. [CrossRef] [PubMed]
4. Tsuchida, Y.; Ito, S.; Fukui, M. Wireless capsule endoscopy: A new tool for cancer screening in the colon with deep-learning-based polyp recognition. *Proc. IEEE* **2019**, *108*, 178–197.
5. Jia, Z.; Yan, G.; Zhu, B. Portable wireless power transmission system for video capsule endoscopy. *J. Med. Eng. Technol.* **2014**, *38*, 351–358.
6. Han, D.; Yan, G.; Wang, Z.; Jiang, P.; Liu, D.; Zhao, K.; Ma, J. The modelling, analysis, and experimental validation of a novel micro-robot for diagnosis of intestinal diseases. *Micromachines* **2020**, *11*, 896. [CrossRef] [PubMed]
7. Basar, M.R.; Ahmad, M.Y.; Cho, J.; Ibrahim, F. An improved wearable resonant wireless power transfer system for biomedical capsule endoscope. *IEEE Trans. Ind. Electron.* **2018**, *65*, 7772–7781. [CrossRef]
8. Lenaerts, B.; Puers, R. Inductive powering of a freely moving system. *Sens. Actuators A Phys.* **2005**, *123*, 522–530. [CrossRef]
9. Ahmed Khan, S.; Ali, A.; Shiyou, Y.; Tong, J.; Guerrero, J.M. Optimized design of embedded air coil for small satellites with various dimensions. *J. Aerosp. Inf. Syst.* **2021**, *18*, 269–279. [CrossRef]
10. Yang, Y.; Xie, X.; Li, G.; Huang, Y.; Wang, Z. A combined transmitting coil design for high efficiency WPT of endoscopic capsule. In Proceedings of the 2015 IEEE International Symposium on Circuits and Systems (ISCAS), Lisbon, Portugal, 24–27 May 2015; pp. 97–100.
11. Liu, T.; Schnabel, A.; Voigt, J.; Sun, Z.; Li, L. A three-step model for optimizing coil spacings inside cuboid-shaped magnetic shields. *AIP Adv.* **2020**, *10*, 115004. [CrossRef]
12. Basar, M.R.; Ahmad, M.Y.; Cho, J.; Ibrahim, F. Stable and high-efficiency wireless power transfer system for robotic capsule using a modified *Helmholtz coil*. *IEEE Trans. Ind. Electron.* **2017**, *64*, 1113–1122. [CrossRef]
13. Xu, C.; Zhuang, Y.; Huang, Y.; Zhou, J. Against Misalignment Wireless Power Transfer System Using a Modified Helmholtz Coil. In Proceedings of the URSI GASS 2020, Rome, Italy, 28 August–4 September 2021.
14. Meng, Y.; Wang, Z.; Jiang, P.; Wang, W.; Chen, F.; Yan, G. Optimization and analysis of Helmholtz-like three-coil wireless power transfer system applied in gastrointestinal robots. *J. Power Electron.* **2020**, *20*, 1088–1098. [CrossRef]
15. Han, D.; Yan, G.; Kuang, S.; Wang, W.; Zhao, K. Preliminary Study on a Three-coil Wireless Power Transfer System for Endoscope Micro-robot of Intestinal Diagnosis: Design, Optimization and Validation. *J. Electr. Eng. Technol.* **2022**, *17*, 2213–2224. [CrossRef]
16. Gao, J.; Yan, G.; Shi, Y.; Cao, H.; Huang, K.; Gao, H.; Liu, J. Analysis of connection way of a three-dimensional receiving coil onboard a capsule robot for wireless power transmission. *Prog. Electromagn. Res. M* **2019**, *78*, 39–48. [CrossRef]
17. Zhang, Z.; Yuan, C.; Gao, J.; Gao, C.; Zhou, A.J. Comparison of the Uniformity and Efficiency of the Square and Circular Helmholtz Coils for Wireless Power Transmission System. *Prog. Electromagn. Res. Lett.* **2021**, *97*, 131–140. [CrossRef]
18. Zhu, B.; Yan, G.; Jia, Z.; Shi, Y. Portable wireless power transmission system of a video capsule endoscopy: Design and realization. In Proceedings of the 2012 International Conference on Biomedical Engineering and Biotechnology, Macau, Macao, 28–30 May 2012; pp. 409–412.
19. Zarifi, T.; Maunder, A.; Moez, K.; Mousavi, P. Tunable open ended planar spiral coil for wireless power transmission. In Proceedings of the 2015 IEEE International Symposium on Antennas and Propagation & USNC/URSI National Radio Science Meeting, Vancouver, BC, Canada, 19–24 July 2015; pp. 105–106.
20. Cheah, W.C.; Watson, S.A.; Lennox, B. Limitations of wireless power transfer technologies for mobile robots. *Wirel. Power Transf.* **2019**, *6*, 175–189. [CrossRef]

21. Fang, T.; Wu, X. A survey of video capsule endoscope system based on wireless energy transfer technology. In *MATEC Web of Conferences*; EDP Sciences: Sanya, China, 2020; Volume 309, p. 01007.
22. Cheng, Y.; Chen, G.; Xuan, D.; Qian, G.; Ghovanloo, M.; Wang, G. Analytical modeling of small, solenoidal, and implantable coils with ferrite tube core. *IEEE Microw. Wirel. Compon. Lett.* **2019**, *29*, 237–239. [CrossRef]
23. Tsuchida, Y.; Ito, S.; Fukui, M. Development of magnetic resonant wireless power transfer system robust to position gap. In Proceedings of the 2018 IEEE International Conference on Consumer Electronics (ICCE), Las Vegas, NV, USA, 12–14 January 2018; pp. 1–4.
24. Zhuang, H.; Wang, W.; Zhao, K.; Fei, Q.; Yan, G. Design and Analysis of a Wireless Power Transfer System for Capsule Robot Using an Optimized Planar Square Spiral Transmitting Coil Pair. *Int. J. Med. Robot. Comput. Assist. Surg.* **2022**, *18*, e2399. [CrossRef] [PubMed]